Research Article

Journal of Chemistry Letters
journal homepage: www.jchemlett.com
ISSN (online) 2717-1892 (print) 2821-0123

Theoretical Study of Interaction Between Thiadiazole Derivatives on Fe(110) Surface

Thomas Aondofa Nyijime[1,*], Habibat Faith Chahul[1], Abdullahi Muhammad Ayuba[2], Fater Iorhuna[2]

[1]*Department of Chemistry, Faculty of Physical Sciences, Federal University of Agriculture,PMB 2373, Makurdi, Benue, Nigeria*
[2]*Department Pure and Industrial Chemistry, Faculty of Physical Sciences, Bayero University PMB 3011 Kano, Nigeria*

ARTICLE INFO

Article history:
Received 28 March 2023
Received in revised form 15 July 2023
Accepted 15 July 2023
Available online 10 August 2023

Keywords:
Quench dynamic simulation
Physical adsorption
Iron surface
Thiadiazole molecule
Corrosion inhibitor

ABSTRACT

The theoretical performance of 4-methoxyphenyl-1,3,4-thiadiazole (AMPT), 2-Amino-5-(4-chlorophenyl)-1,3,4-thiadiazole (ACPT) and 2-amino-5-phenyl-1,3,4-thiadiazole (APT) as inhibitors of iron corrosion was assessed with a view of determining the mechanism of the inhibition process. The reactivity of the molecules with the computed descriptors was explored in order to define and correlate calculations that take into account a number of several global descriptors. Results obtained by calculating adsorption or binding energies were in good agreement with the experimentally reported results elsewhere. Regarding the computed adsorption or binding energies, their generally low values inferred that the compounds are poorly adsorbed onto the surface of Fe through Van der Waals forces and as a result obey the mechanism of physical adsorption.
In order to analyze local reactivity parameters, first- and second-order condensed Fukui functions were used. Simulations involving the adsorbed molecules on Fe (1 1 0) surface were carried out through quench dynamic simulations, and the mechanism of physical adsorption was established with 4-methoxyphenyl-1,3,4-thiadiazole (AMPT), which has proven to be a more effective inhibitor on the Fe surface than 2-amino-5-(4-chlorophenyl)-1,3,4-thiadiazole and 2-Amino-5-phenyl-1,3,4-thiadiazole (APT). Fukui indices values revealed that the active sites were found to be located on the molecules heteroatoms (Sulphur and Nitrogen).

1. Introduction

Metals corrode when they come into contact with oxygen, hydrogen, and their immediate environment, which results in the loss of form, shape, strength, malleability, lustre and durability. In addition, there are other negative effects of corrosion on the environment, such as the loss of life from accidents caused by faulty metal parts, high production costs brought on by high maintenance expenses, and property loss [1-2]. Therefore, it becomes essential to stop, slow down, and prevent this harmful process. Numerous strategies for preventing, protecting from, and limiting corrosion have been described by researchers, taking into account the potential negative effects on the environment as well as cost effectiveness. Many chemicals have been modelled for their corrosion inhibitive potentials in order to limit the harmful consequences of metal corrosion. Recently, the use of pertinent compounds, the majority of which are heterocyclic in nature, as corrosion inhibitors has been accepted. These compounds might be either existing chemicals or extracts from promising plant parts. These heterocyclic compounds or extracts contains polar functional groups and conjugated double bonds as well as organic compounds with polar groups including nitrogen, sulphur and oxygen atoms [3-4]. These substances can adhere to the metal surface, partially obstructing the active sites, slowing the pace of corrosion. Thiadiazole has been reported as a possible metal inhibitor among other nitrogen and sulphur containing compounds [5-6]. The majority of the research work is focused on the use of common inhibitors of different derivatives of compounds such as aminothiazoles [7], benzotriazoles [8–10], thioimidazole

* Corresponding author. Tel.: +2347030874660; e-mail: thomasnyijime@gmail.com
https://doi.org/ 10.22034/JCHEMLETT.2023.391124.1110

[11], and mercapto-5-triazole [12], which have been employed as prospective inhibitors for metal corrosion. The utilization of organic compounds containing nitrogen and sulphur as corrosion inhibitors could be carefully studied in light of the great behaviour of these compounds as corrosion inhibitors, since the necessity to continuously search for more anti-corrosive agents remains crucial [13- 14].

Uncertainty surrounds the interactions between inhibitors and metal substrates. Therefore, a molecular level understanding of metal-inhibitor interactions on iron is highly desired as it may help in the development of inhibitor systems with better characteristics.

The association between molecular structure and corrosion-inhibiting capabilities has been studied successfully over the past several decades using quantum chemistry, and significant progress has been made [15–19]. Humans now have a thorough understanding of the process underlying corrosion inhibition. Nyijime and Iorhuna used the HOMO method to compute the structures of compounds containing N, they found that the electronic density and highest occupied molecular orbital (HOMO) energy level of the active group were related to the effectiveness of the inhibition [28]. However, quantum chemistry computing techniques like ab initio and semi-empirical methods are computationally expensive and are often only used for systems with fewer than 100 atoms or tiny molecules. Modeling massive systems with dozens of metal atoms and hundreds of solvent molecules is not practical. Only a few studies have examined how inhibitors interact with metal surfaces using the molecular dynamics (MD) method [15, 16]. MD is frequently used to analyze the interactions of phase interfaces [15, 17].

It is imperative to fully comprehend and describe the interactions between the inhibitor molecules and the metal surfaces in order to be able to identify new and potent corrosion inhibitors. Theoretical methods can be employed extremely effectively in analyzing these interactions. Density functional theory (DFT) has been used both independently [15–19] and in conjunction with experiments [20–22] to predict the molecular and structural properties of molecules practically in every area of materials research exploring DFT simulations. This study examined the corrosion-inhibitory potential of thiadiazole derivatives. The structures of the 1,3,4-thiadiazole derivatives employed in this investigation whose studied have already been reported [23].

2. Result and Discussion

2.1 Frontier molecular orbitals

It has been observed that the reactivity of molecules is entirely determined by the electronic distribution of the HOMO and LUMO frontier molecular orbitals of the interacting species [24].

To accurately determine the molecules molecular reactivity, it is essential to examine the orbital distribution of the molecules under investigation. The energy of LUMO is related with the ability to absorb electron, HOMO is associated with the ability to donate electrons [25].

Figure 1 displays the structures of the optimized molecules as well as their HOMO and LUMO distribution. For AMPT, APT and ACPT whose structures are all made of either one or two phenyl groups in addition to the thiadiazole moiety, both HOMO and LUMO orbitals were found on the delocalized phenyl group but either on the thia or diazole functional groups made of sulphur, nitrogen, chlorine and oxygen heteroatoms. The HOMO and LUMO orbitals are evenly distributed throughout the thiadiazole molecules in Figure 1, it is clear that both the sulphur, chlorine, oxygen and nitrogen atoms in the molecule have the capacity to contribute electrons to Fe(1 1 0) and as well accept electrons from Fe(1 1 0) through back bonding to create feedback bonds. All of these molecules have a planar structure and a favorable orientation for adsorption on the surface of iron.

2.1.2. Frontier orbital energies

In Table 1, the Outermost orbital energies of the three investigated inhibitors were displayed. These energies were determined using quantum chemical calculations using the BIOVIA Inc Material Studio software 8.0 programs [26].

The parameters being studied were those related to quantum parameters, including $_{E}$HOMO, $_{E}$LUMO, energy gap (ΔE), dipole moment (μ), electronegativity (χ), global hardness (η), global softness (**σ**), and fraction of electron transfer (ΔN). The $_{E}$HOMO value primarily refers to a molecule capacity to denote electrons. The ability of the molecules to donate electrons will be stronger when the $_{E}$HOMO values are higher [27-28]. The table shows that the $_{E}$HOMO of the three inhibitors under study follow the order ACPT>APT>AMPT, which is inconsistent with the inhibition efficiencies that have been obtained experimentally [23]. These changes in additional functional groups present in the molecules under study besides the thiadiazole moiety may be the cause of the variation in the eigen values of the $_{E}$HOMO.

Also, the results demonstrate that the compounds all have equivalent $_{E}$HOMO and $_{E}$LUMO values, which is not at all surprising given that all of the molecules share the same functional groups that make up the HOMO and LUMO, which can result in similar adsorption characteristics.

The $_{E}$LUMO designates the molecular orbitals that are vacant and available for any given electrons. The ability

of $_E$LUMO to receive electrons increases with decreasing $_E$LUMO values [5-7]. Table 1 shows the values of $_E$LUMO, which are noticeably lower in the following order: ACP>APT>ACPT. Moreover, this does not seem to be in line with the experimental findings reported by Yadav et al. [23]. The difference in energy between HOMO and LUMO (energy gap (ΔE)) demonstrates the molecule reactivity to the metal surface [26-28]. When ΔE decreases, the molecule becomes more reactive because less energy is required to remove an electron from the least-occupied molecular orbital [27-28].

The ability of electrons to flow will therefore be easier, more polarizable, and better the smaller the energy gap. The energy gap follows the trends ACPT<AMPT<APT as can also be seen in table 1.The polarity of the polar covalent bond is related to the dipole moment on the other. In the current work, the dipole moment declines in a manner resembling that of $_E$HOMO, $_E$LUMO, and ΔE.

There is comparatively little consistency between the current theoretical findings and the previously reported experimental findings [23].

The inverse of chemical hardness ($\sigma = 1/\eta$) is the definition of global softness, which is the polarizability measure [29-31]. Since metallic bulks are softer than neutral metallic atoms, the theoretical value of electronegativity and hardness of bulk iron are 7.0 eV and 0 respectively by assuming that for a metallic bulk I = A [32]. According to Nyijime et al.

[26], the method of back donating is encouraged if the value of global hardness is positive. In summary, we can say that the interaction of the inhibitor molecules with the iron surface involves the transfer of charge from inhibitor molecules to iron metal and vice versa based on the data shown in table 1.

The values of global hardness are positive and vice versa. In addition, the amount of electrons moved (ΔN) was determined and shown in Table 1. Results obtained indicate that the electron donation-induced inhibition efficiency matches that of Lukovits' work [33].

If ΔN<3.6, the electron-donating capacity of these inhibitors to donate electrons to the metal surface improves, enhancing the efficiency of inhibition.

Hence, the best inhibitor is related with the largest fraction of electrons transported, whereas the inhibitor with the lowest inhibition efficiency is associated with the lowest fraction. As all of the molecules under study have ΔN values lower than 3.6, it is determined that the earlier example holds true for all of them.

2.1.3. Fukui functions

In order to identify the areas of local reactivity of the investigated inhibitor compounds, Fukui indices have been examined. The Fukui indices show which parts of the molecules are reactive to attacks from electrophiles, nucleophiles, and radicals. Only electrophilic and nucleophilic points of attack on the molecules under examination in our study were given attention. The inhibitor molecules may attach to the metal surface through electrostatic attraction, electron transfer, or a combination of the two.

It is crucial to look into the interactions active sites in order to possibly explain their nature or mechanism [26-29].

The maximum threshold values of f_k^+ and f_k^- governs these nucleophilic and electrophilic assaults.

Atoms or regions where the value of f_k^+ is highest are the favored locations for nucleophilic assaults, and electrophilic attacks are preferred when the value of f_k^- is highest. The computed Fukui function values for the compounds under study are shown in Table 2.

As can be observed from table 2, these compounds Fukui functions varied only little with respect to the length of the alkyl chain, suggesting that the local reactivity of these molecules was unaffected by the alkyl chain length. It was found that the f^+ of S(1) atoms on the thiadiazole ring was the highest for these compounds by comparing the Fukui indices of the three molecules in Table 2.

This implies that S(1) atoms, which are nucleophilic reactive sites, have the capacity to absorb electrons from metal surfaces and use them to create back-donating bonds. When it comes to f¯, S(1) atoms on the thiadiazole ring and N(2) atoms on electrophilic attacks have higher values, indicating that they are more likely to provide electrons to metal surfaces so that coordinate bonds can form.

The S(1) atom in the sulphur functional group on the phenyl substituent is the target of a nucleophilic attack on the AMPT molecule, while the N(14) atom in the azole functional group is the target of an electrophilic attack. Both APT and ACPT target the azole functional group's S(1) atom nucleophilically, whereas the nucleophilic attacks are made on the N(3) and N(13) atoms, respectively.

In essence, it may be assumed that nucleophile sites would be preferred for absorption: Sulfur atoms and the electrophile sites are nitrogen atoms, which increases the stability and efficiency of the absorption.

The computed percentage of the second-order Fukui function for the compounds under investigation is shown in Table 3 while their graphical representations are shown in Figure 2.

Table 3 results demonstrate that for both the Mulliken and Hirshfeld charges for AMPT, APT, and ACPT, 100% of the items in Figure 2 had positive values for the Fukui second order function (f2 > 0).

The second order Fukui functions of the three compounds show that they are both nucleophilic in terms of their total reactivity.

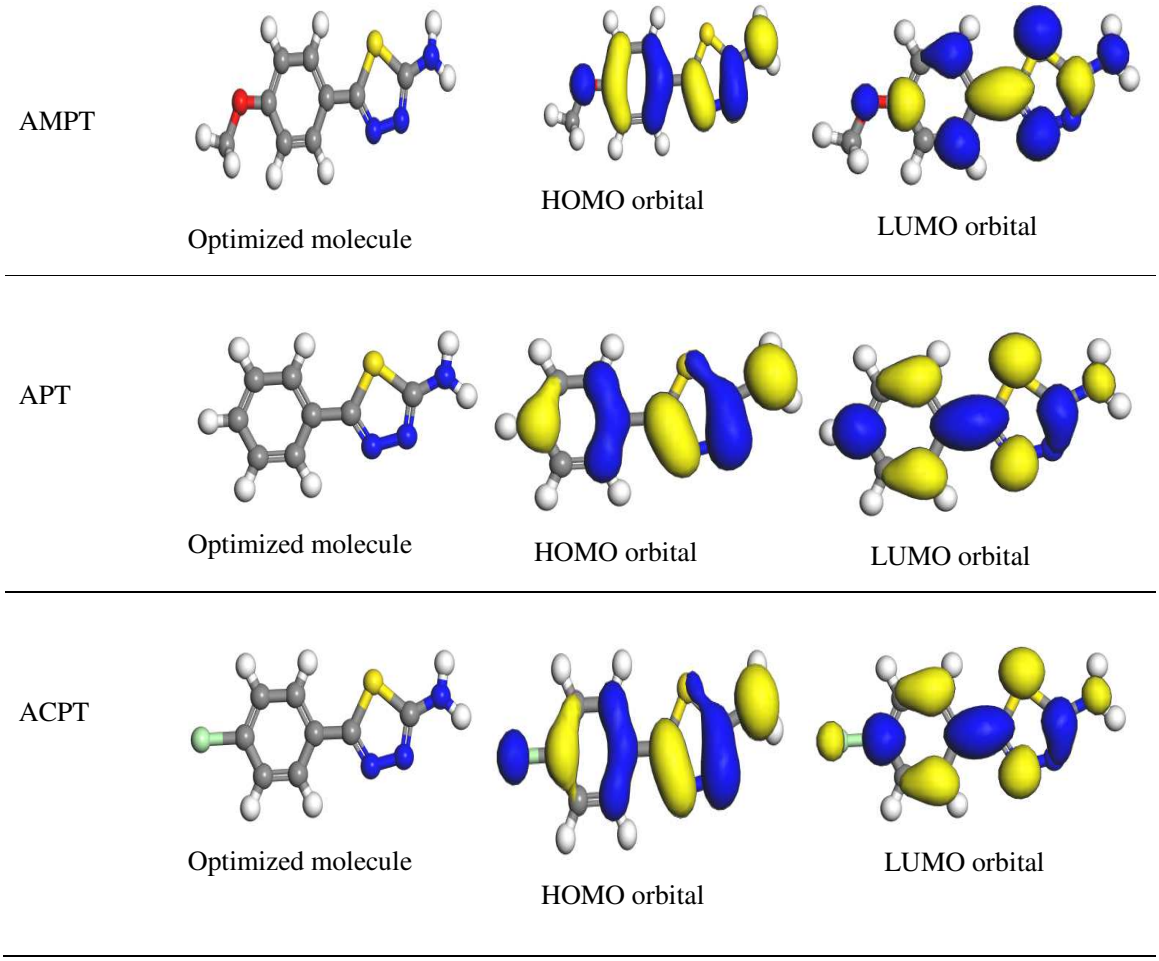

Figure 1: 3D Snap shots of some structural and electronic properties of the thiadiazole derivatives in aqueous phase

Table 1: Values of structural and electronic properties of the thiadiazoles derivatives

Inhibitor	E_{HOMO}(eV)	E_{LUMO}(eV)	ΔE(eV)	μ(Debye)	I=-E_{HOMO}	A=-E_{LUMO}	χ	η	σ	ΔN
AMPT	-5.29	-2.36	2.93	2.54	5.29	2.36	3.83	1.47	0.68	1.08
APT	-5.49	-2.52	2.97	2.02	5.49	2.52	4.01	1.49	0.67	1.00
ACPT	-5.50	-2.63	2.87	2.85	5.50	2.63	4.07	1.44	0.69	1.02

Table 2: Calculated Fukui function of thiadiazole derivatives

Compound	Atom	Nucleophilic attack (+)		Atom	Electrophilic attack (-)	
		Mulliken	Hirshfield		Mulliken	Hirshfield
AMPT	S(1)	0.177	0.154	S(1)	0.098	0.079
	N(4)	0.096	0.105	N(14)	0.100	0.096
APT	S(1)	0.160	0.138	S(1)	0.137	0.111
	N(4)	0.099	0.105	N(3)	0.117	0.122
ACPT	S(1)	0.156	0.138	S(1)	0.122	0.095

	N(4)	0.094	0.103	N(13)	0.129	0.121

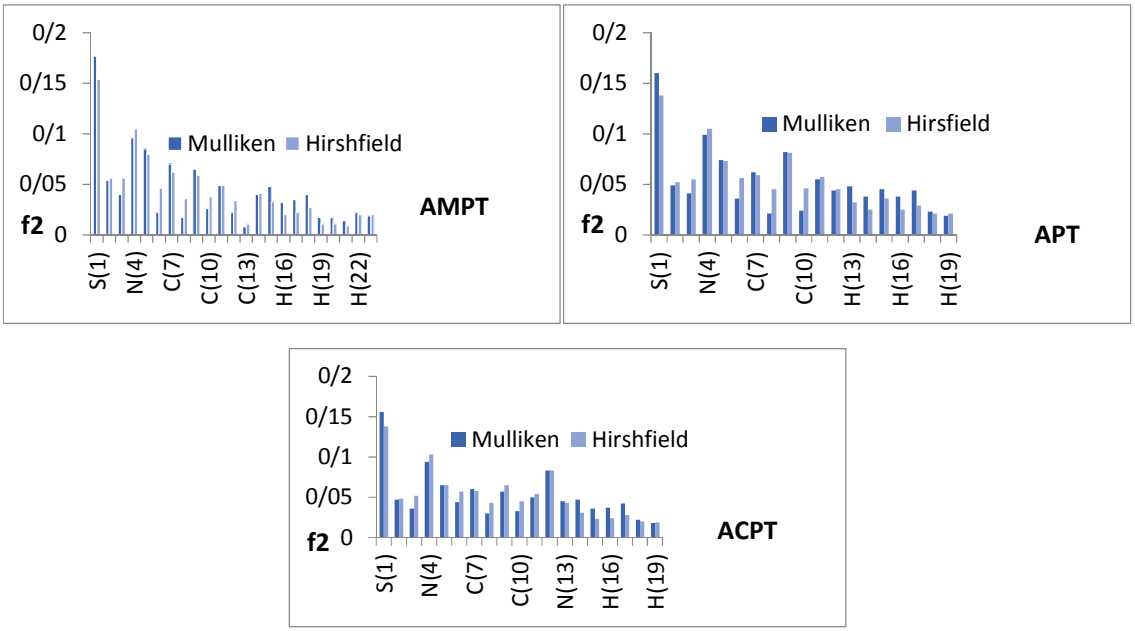

Figure 2: Graphical representation of second-order Fukui function of the studied compounds

Table 3: Calculated percentage of second- order Fukui function of the studied inhibitor molecules

	Nucleophilic (F^+%)		Electrophilic (F^- %)	
Molecule	**Mulliken**	**Hirshfield**	**Mulliken**	**Hirshfield**
AMPT	100	100	100	100
APT	100	100	100	100
ACPT	100	100	100	100

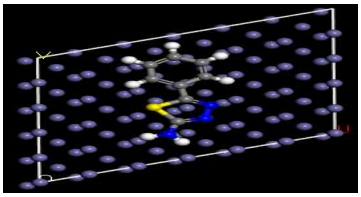

Single AMPT Adsorbed Molecule (Top View)

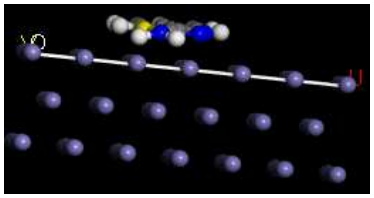

Single AMPT Adsorbed Molecule (Side View)

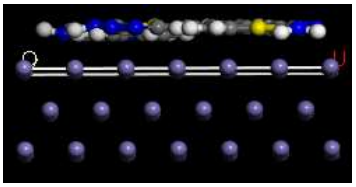

Many AMPT Adsorbed Molecules (Side View)

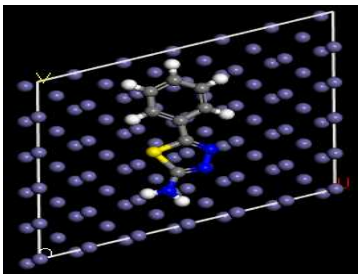

Single APT Adsorbed

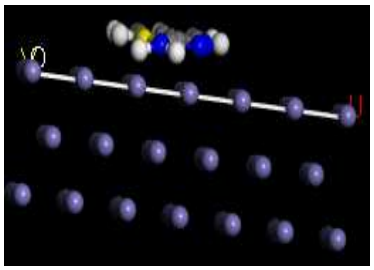

Single APT Adsorbed Molecule

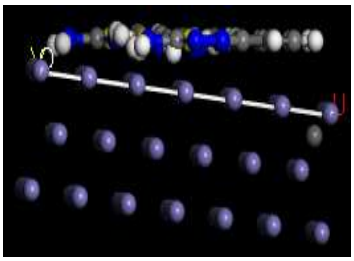

Many APT Adsorbed Molecules (Side View)

Molecule (Top View) (Side View)

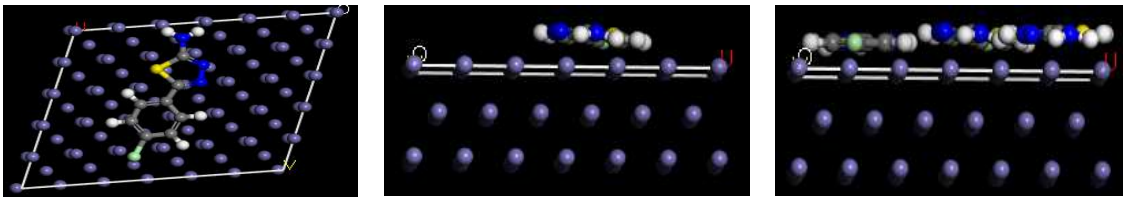

Single ACPT Adsorbed Molecule (Top View) | Single ACPT Adsorbed Molecule (Side View | Many ACPT Adsorbed Molecules (Side View)

Figure 3: Snap shots of the adsorbed thiadiazole molecules on Fe(110) surface.

Table 4: Calculated molecular dynamic simulation parameters for the studied thiadiazoles derivatives

	Inhibitors molecules		
Properties (kcal.mol^{-1})	AMPT	APT	ACPT
Total kinetic energy	13.96±6.9	12.51±6.5	13.41±5.6
Total potential energy	-51.77±0.0	-49.03±0.1	-58.29±0.0
Energy of the molecule	-66.16±0.1	-40.92±0.0	-38.84±0.0
Energy of Fe(110) surface	0.00±0.00	0.00±0.00	0.00±0.00
Adsorption energy	-97.98±0.0	-89.95±0.1	-97.14±0.0
Binding energy	97.98	89.95	97.14

2.2 Molecular dynamic simulation

Molecular dynamic simulation can be used to determine how the inhibitor molecule adsorbs on the metal surface [27]. Modelling the interactions between the inhibitor molecules and the surface of the Fe(110) crystal allowed one to replicate the adsorption of the investigated inhibitor molecules on mild steel. Fig. 3 displays a snapshot of the equilibrium configurations of the simulated systems. Table 4 contains the calculated and reported key energy parameters of the systems. Greater binding or adsorption energies imply a stronger ability for the inhibitor to bind, and thus, higher inhibitive effectiveness [34]. The fact that the ACPT molecule in Table 3 has the highest adsorption or binding energy value suggests that it is more likely than other inhibitors to adsorb on the surface of the iron atom, leading to a stronger inhibitive effect. Moreover, the adsorption or binding energies of AMPT and APT are comparatively higher. According to the data obtained, the three thiadiazole molecules adsorption or binding energies have the following trend: ACPT>AMPT>APT, suggesting that the effectiveness of these thiadiazole molecules' inhibition improves with the length of their alkyl chains. This outcome is fairly consistent with the experimental value reported by Yadav et al. [23]. The number of available adsorption sites on the molecules, the development of metallic complexes, the heteroatoms' ionization potentials, their charge densities, polarity, molecular size, and the way the molecules interact with the Fe surface are just a few of the variables that may affect the order of decreasing inhibition performances [23]. It can also be seen that the ACPT molecule is more efficient than APT. Because of its three potential functional groups—C-O, C-S, and C-N—which have been shown using Fukui indices to improve the adsorption of the molecule on Fe surface—AMPT was shown to have the highest adsorption or binding energy and is, thus, a better inhibitor of Fe corrosion.

3. Computational details

3.1 Methods

All geometric calculations, simulations and theoretical calculations were carried out using the BIOVIA Inc Material Studio software 8.0 programs. After optimizations, quantum chemical parameters were calculated using the B3LYP functional with DND basis set in DMol3 package in aqueous phase model of the Density functional theory (DFT) [35-36]. Geometry optimization and exchange correlations are treated using hybrid B3LYP [28] and full optimization is performed with DNP basis set, which is well accepted to provide accurate geometry and electronic properties of molecules.

The parameters that provide information about molecular reactivity, such as the energy of the highest occupied molecular orbital (EHOMO), lowest unoccupied molecular orbital (ELUMO), electronegativity (χ), ionization potential (IP), electron affinity (EA), hardness (η), softness (σ), and local ones such as the Fukui function f(r), were evaluated

using Koopman's theorem (Equations 1-8) as earlier reported [37].

$IP = -E_{HOMO}$ (1)

$EA = -E_{LUMO}$ (2)

$\Delta E = E_{LUMO} - E_{HOMO}$ (3)

$\chi = \frac{IP+EA}{2} = -\frac{E_{LUMO}+E_{HOMO}}{2}$ (4)

$\eta = \frac{IP-EA}{2} = -\frac{E_{LUMO}-E_{HOMO}}{2}$ (5)

$\Sigma = \frac{1}{\eta}$ (6)

$f_K^+ = q_K(N+1) - q_K(N)$ (7)

$f_K^- = q_K(N) - q_K(N-1)$ (8)

Equation (9) was used to calculate the fraction of electrons that transferred from the inhibitor molecule to the surface of the Fe metal [38].

$\Delta N = \frac{(\chi Fe - \chi inh)}{2(\eta Fe + \eta inh)}$ (9)

Where χ_{Fe} and χ_{inh} stand for the absolute electronegativity of iron (Fe) and the inhibitor molecule (inh), respectively, and η_{Fe} and η_{inh} stand for the absolute hardness of iron (Fe). A theoretical value for the electronegativity of bulk iron was utilized as $\chi Fe=7$ eV and a global hardness of $\eta Fe=0$, by assuming that for a metallic bulk IP=EA since they are softer than the neutral metallic atoms [38]. The contrast between nucleophilic and electrophilic processes defines the derivative of the second-order Fukui function (f2). If $f^2(r) > 0$, site k favors a nucleophilic assault; if $f^2(r) = 0$, site k favors an electrophilic assault. Thus, $f^2(r)$ may serve as a selectivity signal for electrophilic or nucleophilic attacks.

The Fukui function is $f(r) = f^+ - f^- = f^2$ (10)

Molecular dynamics (MD) simulation of the interaction between a single molecule and the Fe surface was performed using Forcite quench MD in Material Studio (MS) Modeling 7.0 software to sample many different low-energy minima and to determine the global energy minimum [4, 27-29]. In order to determine an average global minimum, this aims to sample five different low energy minima of the quenched dynamics [39]. Because of its stability and more densely packed atoms, the cleaved Fe(110) plane was chosen out of all the possible Fe surfaces [40]. The simulations were run using the clever algorithm and the condensed-phase optimized molecular potentials for atomistic simulation studies (COMPASS) force field on a 6 x 5 supercell of the Fe(110) surface. The constructed Fe slab was significantly relative larger than the molecule to fully accommodate the adsorbed molecule in order to prevent potential molecular edging effects that may occur during the docking process. Using the NVE ensemble, 5ps simulation period and 1 fs time step, the temperature of the simulation was set to be at 350K and the completely optimized molecule and Fe surface was utilized for the docking process. Every 250 steps, the system were quenched, and the optimum Fe surface atoms were tightly restricted. Equation (10) was utilized [41-42] to obtain the adsorption (Eads) and (BE) binding energies of the single molecule adsorption on the Fe(110) surface, allowing access to linking them to inhibitory efficiencies.

$Eads = -BE = E_{complex} - (E_{Fe} + E_{inhibitor} +)$ (11)

Where, $E_{complex}$ is the total energy of the Fe surface and inhibitor, E_{Fe} is the energy of the Fe surface without the inhibitor, and $E_{inhibitor}$ is the energy of the inhibitor without the Fe surface.

4. Conclusion

Our findings were used to predict the inhibitory characteristics of thiadiazole compounds against the corrosion of iron metal using quantum chemical calculations and molecular dynamic simulations. It is clear that the resulting results were in strong agreement with those reported experimentally. Also, it was determined that the thiadiazole molecules relatively low adsorption or binding energy on the Fe surface indicated the physical adsorption mechanism. Comparing APT to the other two compounds, which are more likely to be effective as corrosion inhibitors on Fe surfaces, it was discovered that APT had the lowest inhibitory efficiency in terms of adsorption or binding energies.

Acknowledgements

The authors wish to acknowledge the contribution of Dr. Abdullahi Muhammad Ayuba of the department of pure and industrial chemistry, Bayero University, Kano, Nigeria for the installation of the BIOVIA Material Studio 8.0 software.

References

[1] W. Sun and S. Nesic: A mechanistic model of H2S corrosion of mild steel, Paper No. 07655, NACE International corrosion conference & Expo. Houstan, Texas, 2007.

[2] W. Baran, E. Adamek, J. Ziemia-nska, Effects of the presence of sulfonamides in the environment and their influence on human health. *J. Hazard. Mater.*, 196 (2011) 1–15.

[3] A. Mishra, C. Verma, V. Srivastava, H. Lgaz, M.A. Quraishi, E.E. Ebenso, I. Chung, "Chemical, electrochemical and computational studies of newly synthesized novel and environmental friendly heterocyclic compounds as corrosion inhibitors for

mild steel in acidic medium, *Journal of Bio- and Tribo-Corrosion* 2018, 14, 32. doi.org/10.1007/s40735-018-0147-y.

[4] S. Kaya, C. Kaya, L. Guob, F. Kandemirli, B. Tüzün, İ. Uğurlu, L. H. Madkour, M. Saraçoğlu, Quantum chemical and molecular dynamics simulation studies on inhibition performances of some thiazole and thiadiazole derivatives against corrosion of iron, *Journal of Molecular Liquids*, 219 (2016) 497–504.

[5] N. A.Wazzan, I.B. Obot, S. Kaya, Theoretical modeling and molecular level insights into the corrosion inhibition activity of 2-amino-1,3,4-thiadiazole and its 5-alkyl derivatives, *Journal of Molecular Liquids*, 221 (2016) 579–602.

[6] J. Saranya, F. Benhiba, N. Anusuya, A. Zarrouk, S. Chitra, Thiazolo thiadiazole derivatives as anti-corrosion additives for acid corrosion, *Chemical Data Collections*, 26 (2020) 100358.

[7] D. D. N. Singh, M. M. Singh, R. S. Chaudhary, and C. V. Agarwal, Inhibitive effects of isatin, thiosemicarbazide and isatin-3-(3-thiosemicarbazone) on the corrosion of aluminium alloys in nitric acid, *Journal of Applied Electrochemistry*, 10(1980) 587–592, 1980.

[8] I. A. Ammar and S. Darwish, Effect of some ions on inhibition of the acid corrosion of fe by thiourea, *Corrosion Science*, 9(1967) 579–596.

[9] S. K. Shukla and E. E. Ebenso, Effect of condensation product of thiosemicarbazide and phenyl isothiocynate on corrosion of mild steel in sulphuric acid medium, *International Journal of Electrochemcal Science*, 7(2012) 12134–12145.

[10] R. M. Souto, V. Fox, M. M. Laz, M. P´erez, and R. S. Gonz´alez, some experiments regarding the corrosion inhibition of copper by benzotriazole and potassium ethyl xanthate, *Journal of Electroanalytical Chemistry*, 411(1996) 161–165.

[11] E. Otero and J. M. Bastidas, Cleaning of two hundred year-old copper works of art using citric acid with and without benzotriazole and 2-amino-5-mercapto-1,3,4-thiadiazole," *Materials and Corrosion*, 47(1996) 133–138.

[12] W.Z. Li, Y. Zhang, L. Zhai, W. Ruan, L.W. Zhang, Corrosion Inhibition of N80 Steel by Newly Synthesized Imidazoline Based Ionic Liquid in 15% HCl Medium: Experimental and Theoretical Investigations, *International Journal of Electrochemical Science.* 15(2020) 722–739

[13] A. Popova, M. Christov, S. Raicheva, E. Sokolova, Adsorption and inhibitive properties of benzimidazole derivatives in acid mild steel corrosion, *Corros. Sci*. 46 (2004) 1333e1350, https://doi.org/10.1016/j.corsci.2003.09.025..

[14] X. He, J. Mao, Q. Ma, Y. Tang, "Corrosion inhibition of perimidine derivatives for mild steel in acidic media: Electrochemical and computational studies" *Mol. liq*, (2018) DOI:10.1016/j.molliq.2018.08.021.

[15] M.E. Belghiti, A. Dafali, Y. Karzazi, M. Bakasse, H. Elalaoui- Elabdallaoui, L.O. Olasunkanmi, E.E. Ebenso, Computational simulation and statistical analysis on the relationship between corrosion inhibition efficiency and molecular structure of some hydrazine derivatives in phosphoric acid on mild steel surface, *Appl. Surf. Sc*i. 491 (2019) 707e722, https://doi.org/ 10.1016/j.apsusc.2019.04.0125.

[16] M. Jayalakshimi, V.S. Muralidharan, Correlation between structure and inhibition of organic-compounds for acid corrosion of transition-metals, *Indian J. Chem. Technol.* 5 (1998) 16e28. http://cecri.csircentral.net/id/eprint/2527.

[17] J. Frau, D. Glossman-Mitnik, Conceptual DFT descriptors of amino acids with potential corrosion inhibition properties calculated with the latest Minnesota density functionals, *Front.Chem*. 5 (2017) 16, https://doi.org/10.3389/fchem.2017.00016.

[18] M. E. Belghiti, Y. El Oudadi, S. Echihi, A. Elmelouky, H. Outada, Y. Karzazi, M. Bakasse, C. Jama, F. Bentiss, A. Dafali, Anticorrosive properties of two 3,5-dissubstitud-4-amino-1,2,4-triazole derivatives on copper in hydrochloric acid environment: Ac impedance, thermodynamic and computational investigations. *Surface Interface* 21 (2020) 100692. doi: 10.1016/j.surfin.2020.100692. .

[19] E. Alibakhshi, M. Ramezanzadeh, G. Bahlakeh, B. Ramezanzadeh, M. Mahdavian, M. Motamedi, Glycyrrhiza glabra leaves extract as a green corrosion inhibitor for mild steel in 1 M hydrochloric acid solution: experimental, molecular dynamics, monte carlo and quantum mechanics study. *J Mol Liq* 255(2018) 185–198.

[20] D. Alokdut, K.S. Sourav, A. Utpal, B. Priyabrata, S. Dipankar, Effect of substitution on corrosion inhibition properties of 2- (substituted phenyl) benzimidazole derivatives on mild steel in 1M HCl solution: a combined experimental and theoretical approach" *Corros Sci* 123(2017) 256–266.

[21] N. OBoyle, A. Tenderholt, K. Langner, A library for package independent computational chemistry algorithms. *J. Comput. Chem*., 29 (2008) 839–845.

[22] F. Gharibzadeh, E. Vessally, E. Edjlali L, A DFT study on Sumanene, Corannulene and nanosheet as the anodes in Li–ion batteries. *Iran J Chem Chem Eng*., 39 (2020) 51–62.

[23] M. Yadav, P.N. Yadav, U. Sharma, Substituted thiadiazoles as corrosion inhibitors for N80 steel in hydrochloric acid. *Indian Journal of Chemical Technology*, 20(2013) 363-373.

[24] P.O. Ameh, "Electrochemical and computational study of gum *exudates* from *Canarium schweinfurthii* as green corrosion inhibitor for mild steel in HCl solution" *J. Taibah Univ. Sci*.2018, 12, 783 – 795. https://doi.org/10.1080/16583655.2018.1514147

[25] K.M. Zohdy, R.M. El-Sherif, S. Ramkumar, A.M. El-Shamy, "Quantum and electrochemical studies of the hydrogen evolution findings in corrosion reactions of mild steel in acidic medium" *Upstream Oil Gas Technol* 6:100025, 2021.

[26] T.A. Nyijime, H.F. Chahul, A.M. Ayuba, F.Iorhuna, Theoretical Investigations on Thiadiazole Derivatives as Corrosion Inhibitors on Mild Steel. *Advanced Journal of Chemistry-Section A*, 6(2023) 141-154

[27] A.M. Ayuba, T.A. Nyijime, A.S. Muhammad, Density functional theory and molecular dynamic simulation

studies on the corrosion inhibition of some thiosemicarbazide derivatives on aluminum metal. *Journal of Applied Surfaces and Interfaces* 8(2020)7-14

[28] T.A. Nyijime, F. Iorhuna, Theoretical study of 3-(4-hydroxyphenyl)-1-(4-nitrophenyl) prop-2-en-1-one and 3-(4-hydroxyphenyl)-1-phenylprop-2-en-1-one as corrosion inhibitors on mild steel. *Appl. J. Envir. Eng. Sci*. 8(2022) 177-186

[29] N. P. Bellafont, F. Illas, P. S. Bagus, Validation of Koopmans' theorem for density functional theory binding energies. *Physical Chemistry Chemical Physics* 17 (2015) 4015e-4019. doi: 10.1039/C4CP05434B.

[30] L. H. Madkour, I. H. Elshamy, Experimental and computational studies on the inhibition performances of benzimidazole and its derivatives for the corrosion of copper in nitric acid. *International Journal of Industrial Chemistry*, 7 (2016) 195e221. doi: 10.1007/s40090-015-0070-8.

[31] A. A. Khadom, Quantum chemical calculations of someamines corrosion inhibitors/copper Alloy interaction in hydrochloric acid. *Journal of Material and Environmental Science* 8 (2017) 1153e1160. http://www.jmaterenvironsci.com.

[32] V.S. Sastri, J.R. Perumareddi, "Molecular orbital theoretical studies of some organic corrosion inhibitors" *Corrosion*, 53,(1997) 617.

[33] I. Lukovits, E. Kalman, F. Zucchi, Corrosion inhibitors correlation between electronic structure and efficiency. *Corrosion*, 57 (2001), 3-8.

[34] T.A. Salman, K.A. Samawi, J.K. Shneine, "Electrochemical and computational studies for mild steel corrosion inhibition by benzaldehyde thiosemicarbazone in acidic medium" *Port. Electrochim. Acta*. 2019, 37, 241-255. DOI: 10.4152/pea.201904241.

[35] M. Musavi, theoretical study of interaction between Mexiletine drug and pristine, Si-, Ga- and Al-doped boron nitride nanosheet. *J. Chem. Lett*. 3 (2022) 150-158

[36] U. Umar, A. M. Ayuba, Adsorption of SO2 and NO2 on ZrO2 (1 1 0) Surface: Density Functional Theory and Molecular Dynamic Simulation Studies, *J. Chem. Lett*. 3 (2022) 135-143

[37] T. Koopmans, Ordering of wave functions and eigen energies to the individual electrons of an atom. *Physica*, 1 (1993), 104-113.

[38] T. A. Nyijime and A. M. Ayuba, Quantum chemical studies and molecular modeling of the effect of coriandrum sativum L. compounds as corrosion inhibitors on aluminum surface.
Applied Journal of Environmental Engineering Sciences 6(2020) 344-355.

[39] L. O. Olasunkanmi, I. B. Obot, M. M. Kabanda and E. E. Ebenso, Some quinoxalin-6-yl derivatives as corrosion inhibitors for mild steel in hydrochloric acid: experimental and theoretical studies. *Journal of Physical Chemistry C* 119 (2015) 16004-16019. doi: 10.11021/acs.jpcc.5b03285.

[40] L. Guo, X. Ren, Y. Zhou, S. Xu, Y. Gong, S. Zhang, Theoretical evaluation of the corrosion inhibition performance of 1,3-thiazole and its amino derivatives. *Arabian Journal of Chem*istry 10 (2015) 121–130. doi: 10.1016/j.arabjc.2015.01.005

[41] M. K. Awad, Quantum chemical studies and molecular modelling of the effect of polyethylene glycol as corrosion inhibitors of an aluminium surface. *Canadian Journal of Chemistry* 91 (2013) 283-291. doi: 10.1139/cjc.2012-0354.

[42] U. Umaru and A. M. Ayuba, Modeling vitexin and isovitexin flavones as corrosion inhibitors for aluminium metal. *Karbala International Journal of Modern Science* 7(2021) 206-215. doi: 10.33640/2405-609X.311